Journal of Membrane Science 367 (2011) 204–210

Contents lists available at ScienceDirect

Journal of Membrane Science

journal homepage: www.elsevier.com/locate/memsci

A simplified procedure for estimation of mixture permeances from unary permeation data

Rajamani Krishna[a,b,*], Jasper M. van Baten[a]

[a] Van't Hoff Institute for Molecular Sciences, University of Amsterdam, Science Park 904, 1098 XH Amsterdam, The Netherlands
[b] Department of Chemical & Biomolecular Engineering, University of California, Berkeley, Berkeley, CA 94720, USA

ARTICLE INFO

Article history:
Received 18 July 2010
Received in revised form 24 October 2010
Accepted 28 October 2010
Available online 4 November 2010

Keywords:
Permeances
Permeation selectivity
Correlation effects
Adsorption
Maxwell–Stefan diffusion

ABSTRACT

Using the Maxwell–Stefan (M–S) diffusion equations as a basis, we derive simple analytic expression for the estimation of component permeances of mixtures across micro- and mesoporous membranes on the basis of unary permeation data. The analytic procedure uses two simplifying assumptions: (1) downstream pressures are negligibly small in comparison to upstream pressures, and (2) adsorption equilibrium within the pores can be described by Henry law coefficients. Two limiting scenarios are considered in estimating the M–S exchange coefficients, $Đ_{ij}$: (1) correlations negligible, and (2) correlations dominant. In the correlations negligible scenario, the permeances of each component in the mixture equal that of the corresponding pure components. For the correlations dominant scenario, the permeances in the mixture are significantly different from the pure component values; the differences being dictated not only by mobilities of the species within the pores, but also by the adsorption equilibrium. The results of this study underlines the strong influence of diffusional correlations on the mixture permeances and permeation selectivities.

1. Introduction

A wide variety of micro- and mesoporous materials are of potential use in membrane separation applications [1–8]. Examples of microporous materials include zeolites (crystalline aluminosilicates), carbon nanotubes (CNTs), carbon molecular sieves (CMS), metal–organic frameworks (MOFs), zeolitic imidazolate frameworks (ZIFs), and titanosilicates (such as ETS-4, and ETS-10). Examples of mesoporous materials include SBA-16, MCM-41, and Vycor glass.

For modeling n-component mixture diffusion inside either micro- or mesopores, it is commonly accepted that the fundamentally correct approach is to relate the fluxes N_i, defined in terms of the cross-sectional area of the membrane, to the chemical potential gradients $\nabla\mu_i$ by use of the Maxwell–Stefan (M–S) equations [7–11]

$$-\phi\frac{c_i}{RT}\nabla\mu_i = \sum_{\substack{j=1\\ j\neq i}}^{n}\frac{x_jN_i - x_iN_j}{Đ_{ij}} + \frac{N_i}{Đ_i};\quad i = 1, 2, \ldots, n \tag{1}$$

where ϕ represents the fractional pore volume of the porous material, and the concentrations c_i are defined in terms of moles per m^3 of accessible pore volume. The x_i in Eq. (1) are the component mole fractions of the adsorbed phase within the micropores

$$x_i = \frac{c_i}{c_t};\quad i = 1, 2, \ldots, n \tag{2}$$

The $Đ_i$ characterize species i–wall interactions in the broadest sense. In many cases the $Đ_i$ corresponds to the value of the pure component i; consequently this can be estimated from unary permeation data. In some exceptional cases the $Đ_i$ in the mixture can be lower than that of pure components [12–14]. The $Đ_{ij}$ are exchange coefficients representing interaction between components i with component j. At the molecular level, the $Đ_{ij}$ reflect how the facility for transport of species i correlates with that of species j. Conformity with the Onsager reciprocal relations prescribes

$$Đ_{ij} = Đ_{ji} \tag{3}$$

In some of published formulations on multicomponent diffusion in zeolites [15,16], the M–S equations are set up differently using loadings expressed as moles per kg of framework. A detailed comparison of the earlier approaches with the current one, using Eq. (1), is provided by Krishna and Van Baten [9]; see the supplementary material accompanying their paper. There are several important advantages in using the current approach using moles per accessible pore volume, c_i. Firstly, Eq. (1), are applicable equally

* Corresponding author at: Van't Hoff Institute for Molecular Sciences, University of Amsterdam, Science Park 904, 1098 XH Amsterdam, The Netherlands.
Tel.: +31 20 6270990; fax: +31 20 5255604.
E-mail address: r.krishna@uva.nl (R. Krishna).

0376-7388/$ – see front matter © 2010 Elsevier B.V. All rights reserved.
doi:10.1016/j.memsci.2010.10.055

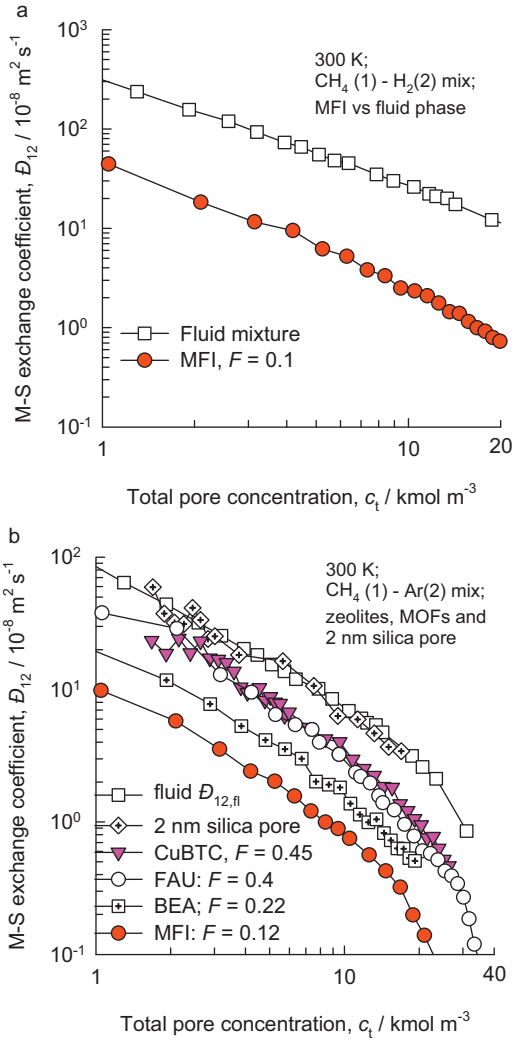

Fig. 1. The M–S binary exchange coefficients $Đ_{12}$, for diffusion of equimolar ($c_1 = c_2$) binary mixtures (a) $CH_4(1)$–$H_2(2)$, and (b) $CH_4(1)$–Ar(2), in zeolites, MOFs, and 2 nm silica pore at 300 K as a function of the total concentration, c_t. The $Đ_{12,fl}$ for binary fluid phase mixture diffusion, obtained from independent MD simulations, are also presented in square symbols.

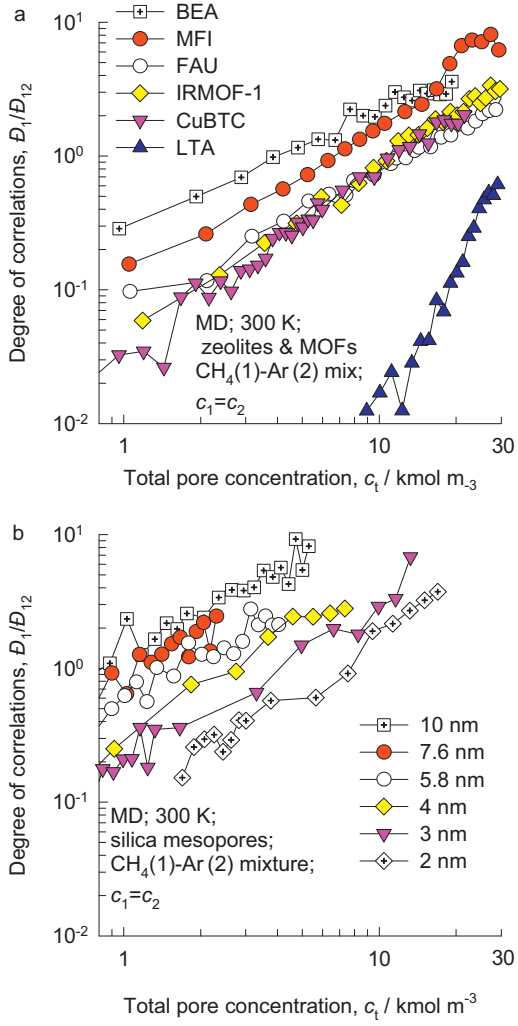

Fig. 2. The degree of correlations, $Đ_1/Đ_{12}$, for $CH_4(1)$–Ar(2) mixture diffusion a variety of (a) zeolites, MOFs, and (b) silica mesopores of different diameters. The data are culled from earlier publications [9,10,16,31].

to micro- and mesoporous materials, as explained in our earlier papers [9,10,17–20]. Furthermore, the use of the current formulation allows a much clearer interpretation of the M–S diffusivities $Đ_{ij}$, that quantify correlation effects. The diffusivities $Đ_{ij}$ are relatable to the corresponding M–S diffusivity in the binary fluid mixture, with species i and j. Within mesopores, the $Đ_{ij}$ can be identified with the corresponding fluid phase diffusivity, $Đ_{ij,fl}$, when compared at the same total molar concentration c_t within the pores. For microporous materials, the $Đ_{ij}$ are lower than the corresponding fluid phase diffusivity by a factor, F, that depends on the degree of confinement within the micropores. To illustrate this, Fig. 1a compares the MD simulated data on $Đ_{12}$ for $CH_4(1)$–$H_2(2)$ mixture diffusion in MFI zeolite with the corresponding diffusivity in a binary fluid mixture, $Đ_{12,fl}$. Within the 0.55 nm pores of MFI zeolite, the $Đ_{12}$ is about a tenth of the value for the corresponding fluid mixture, when compared at the total molar concentration c_t within the pores, i.e. $F = 0.1$. The stronger the degree of confinement, the smaller is the value of F. This is illustrated in Fig. 1b by the MD simulated $Đ_{12}$ data for $CH_4(1)$-Ar (2), in zeolites, MOFs, and 2 nm silica pore. For the 2 nm silica pore, the $Đ_{12}$ is practically the same as the fluid phase $Đ_{12,fl}$. For microporous zeolites and MOFs, the $Đ_{12}$ values are significantly lower. The factor F is higher, relatively speaking, in more open structures such as CuBTC and FAU than within the more constrained pores of MFI zeolite.

One major problem in the calculation of the N_i lies in the proper estimation of the exchange coefficients $Đ_{ij}$. The relative contributions of the first and second right members of Eq. (1) are dictated by the degree of correlations, defined as $Đ_i/Đ_{ij}$. The higher the degree of correlations, the more important is the contribution of the first right member. As a consequence, Eq. (1) becomes more strongly coupled if the degree of correlations is higher. Using experimental data alone, there is no procedure to determine the $Đ_i/Đ_{ij}$. Molecular dynamics (MD) simulations of mixture diffusion in a wide variety of micro- and mesoporous materials show that, depending on the pore size, connectivity, and topology the $Đ_i/Đ_{ij}$ can vary by a few orders of magnitude [6]. As illustration, Fig. 2 presents the MD simulation data for $Đ_1/Đ_{12}$ in $CH_4(1)$–Ar(2) mixtures for a variety of zeolites (BEA (intersecting channels of 0.72 nm and 0.56 nm), MFI (intersecting channels of 0.51 and 0.55 nm), FAU (0.73 nm window opening), LTA (0.41 nm window)), MOFs (CuBTC (0.9 nm window aperture), IRMOF-1 (0.8 nm window opening)), and silica mesopores as a function of the total mixture concentration within the pores, c_t. At $c_t = 10$ kmol m^{-3}, for example, $Đ_1/Đ_{12}$ has the lowest value of 0.01 for LTA that consists of cages separated by narrow windows of 0.41 nm size. The correlations in LTA are low because only one molecule at a time can hop from one cage to the adjoining one.

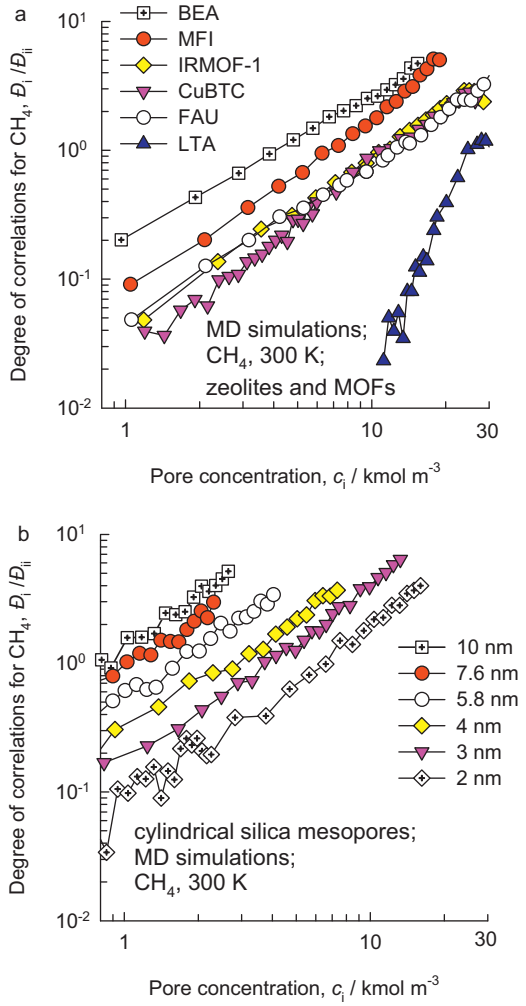

Fig. 3. The degree of correlations, $Đ_i/Đ_{ii}$, for CH_4 diffusion a variety of (a) zeolites, MOFs, and (b) silica mesopores of different diameters. The data are culled from earlier publications [9,10,16,31].

For "open" structures such as CuBTC, IRMOF-1, and FAU, $Đ_1/Đ_{12} \approx 1$. Within the intersecting channel topology of MFI, correlations are still higher and $Đ_1/Đ_{12} \approx 2$. The highest degree of correlations are for mesopores; for example for a 10 nm pore, $Đ_1/Đ_{12} \approx 10$.

For any given material, the $Đ_i/Đ_{ij}$ increases with increasing pore concentration. As the concentration within the pores increases, the jumps of individual molecules become increasingly correlated because the number of vacant sites will decrease, and the probability of unsuccessful jumps will increase.

MD simulations have also shown that the degree of correlations in the mixture can be estimated on the basis of the degree of correlations for the individual pure components, defined by $Đ_i/Đ_{ii}$. Data for pure CH_4 in a variety of zeolites, MOFs, and silica mesopores show that the $Đ_i/Đ_{ii}$ has a similar hierarchy and concentration dependence as for mixture diffusion; see Fig. 3.

In the literature it has been suggested that the exchange coefficient in the mixture can be estimated on the basis of the pure component self-exchange coefficients, $Đ_{ii}$, using an interpolation formula [9]

$$Đ_{12} = (Đ_{11})^{x_1}(Đ_{22})^{x_2} \tag{4}$$

Though this interpolation formula has been verified on the basis of MD simulations [9], the major obstacle to its use in practice is that information on the degree of correlations for pure components are also not accessible experimentally. A different procedure for estimate the exchange coefficient is to relate $Đ_{12}$ to the M–S diffusivity of the corresponding fluid mixture. For diffusion within mesopores, the $Đ_{12}$ can be identified with the corresponding M–S diffusivity for a fluid phase binary mixture [9,10], evaluated at the same total concentration, c_t, as within the pores. For micropore diffusion the $Đ_{ij}$ are lower than the corresponding fluid phase diffusivity by a factor; this factor can be in the range 0.01–1, depending on the degree of confinement [9,10].

The approach taken in the present communication is to develop and analyze limiting scenarios for the degree of correlations. The primary objective is to derive a simplified analytic procedure for the estimation of the steady-state fluxes N_i for two scenarios: correlations negligible and correlations dominant. The derived analytic expressions allow explicit calculation of the N_i from unary permeation data; these serve as "bounding" values. We demonstrate the utility of the developed expressions for screening purposes.

2. Development of simplified analytic expressions

The first step is to re-write Eq. (1) in a more practically useful form. The chemical potential gradients $\nabla\mu_i$ can be related to the more conventional gradients of concentrations within the pores by defining thermodynamic correction factors Γ_{ij}

$$\frac{c_i}{RT}\nabla\mu_i = \sum_{j=1}^{n}\Gamma_{ij}\nabla c_j; \qquad \Gamma_{ij} = \frac{c_i}{p_i}\frac{\partial p_i}{\partial c_j}; \quad i,j = 1,\ldots,n \tag{5}$$

If the adsorption equilibrium is represented by the single-site Langmuir isotherm

$$\theta_i = \frac{c_i}{c_{i,sat}} = \frac{b_i p_i}{1+\sum_{i=1}^{n} b_i p_i}; \quad i = 1,2,\ldots,n \tag{6}$$

the matrix $[\Gamma]$ can be determined by differentiation of Eq. (6).

By defining an n-dimensional square matrix $[B]$ with elements

$$B_{ii} = \frac{1}{Đ_i} + \sum_{\substack{j=1\\ j\neq i}}^{n}\frac{x_j}{Đ_{ij}}; \qquad B_{ij} = -\frac{x_i}{Đ_{ij}}; \quad i,j = 1,2,\ldots,n; \tag{7}$$

the M–S equation (1) can be re-written to relate the fluxes N_i explicitly to the gradients of the concentration gradients using n-dimensional matrices

$$(N) = -\phi[\Delta][\Gamma]\nabla(c) = -\phi[B]^{-1}[\Gamma]\nabla(c) \tag{8}$$

where additionally, we define the square matrix $[\Delta]$

$$[\Delta] = [B]^{-1} \tag{9}$$

For steady-state permeation of mixtures across a membrane, the set of coupled equations (5)–(9) need to be solved numerically in the general case [21]. Explicit analytic expressions are available for some special cases [22].

In proceeding forward with our theoretical development, we shall make two further assumptions: (1) that the downstream partial pressures are negligibly small in relation to the upstream values, and (2) that adsorption equilibrium is describable by a simple Henry's law

$$c_i = K_i p_i; \qquad K_i = b_i c_{i,sat} \tag{10}$$

In the Henry regime, the non-diagonal terms of $[\Gamma]$ vanish.

For steady-state conditions, Eq. (8) can be integrated across the membrane thickness ℓ to obtain the fluxes for binary mixtures explicitly in terms of the partial pressures p_i in the upstream compartment

$$N_1 = \frac{\phi}{\ell}(\Delta_{11}K_1p_1 + \Delta_{12}K_2p_2); \qquad N_2 = \frac{\phi}{\ell}(\Delta_{21}K_1p_1 + \Delta_{22}K_2p_2) \tag{11}$$

In deriving equation (11), the elements of square matrix $[\Delta]$ are assumed to be independent of the adsorbed phase compositions x_i. This is a good assumption to make in the general case

The corresponding expressions for the permeances, defined by

$$\Pi_i \equiv \frac{N_i}{p_i} \tag{12}$$

are

$$\Pi_1 = \frac{\phi}{\ell}\frac{\Delta_{11}K_1p_1 + \Delta_{12}K_2p_2}{p_1}; \qquad \Pi_2 = \frac{\phi}{\ell}\frac{\Delta_{21}K_1p_1 + \Delta_{22}K_2p_2}{p_2} \tag{13}$$

The permeances in the mixture can be calculated explicitly provided we are able to estimate the elements of $[\Delta]$.

We can identify two limiting scenarios. In the correlations negligible scenario we take $Đ_i/Đ_{ij} \to 0$. This simplification yields

$$\Delta_{ii} = Đ_i; \qquad \Delta_{ij}(i \neq j) = 0;$$
$$i, j = 1, 2, \ldots, n; \quad \text{correlations negligible} \tag{14}$$

and Eq. (13) simplifies to yield expressions for the mixture permeances that are equal to the corresponding values for the pure components

$$\Pi_i = \frac{\phi}{\ell}Đ_iK_i \equiv \Pi_i^0; \quad i, j = 1, 2, \ldots, n; \quad \text{correlations negligible} \tag{15}$$

The membrane permeation selectivity, S_{perm}, is

$$S_{perm} = \frac{\Pi_i}{\Pi_j} = \frac{\Pi_i^0}{\Pi_j^0} = \frac{Đ_iK_i}{Đ_jK_j}; \quad \text{correlations negligible} \tag{16}$$

and this can also be determined from unary permeances. Eq. (15) is an expected result. If correlation effects are assumed to be negligible, the permeances in the mixture equal that of the pure components.

At the other extreme we have the correlations dominant scenario $Đ_i/Đ_{12} \gg 1$. In this case the following explicit expressions for $[\Delta]$ can be derived, as shown in previous work [16,17]

$$\Delta_{11} = \Delta_{12} = \frac{c_1}{(c_1/Đ_1) + (c_2/Đ_2)};$$
$$\Delta_{21} = \Delta_{22} = \frac{c_2}{(c_1/Đ_1) + (c_2/Đ_2)}; \quad \text{correlations dominant} \tag{17}$$

Inserting Eq. (17) into (13) yields, after simplification and introduction of the definition of the pure component permeances

$$\Pi_1 = \frac{K_1}{(K_1x_1/\Pi_1^0) + (K_2x_2/\Pi_2^0)};$$
$$\Pi_2 = \frac{K_2}{(K_1x_1/\Pi_1^0) + (K_2x_2/\Pi_2^0)}; \quad \text{correlations dominant} \tag{18}$$

The adsorbed phase mole fractions x_i can be estimated by combining Eqs. (2) and (10). Eq. (18) shows that the permeances in the mixture are directly influenced adsorption equilibrium.

Eq. (18) can be generalized for n-component mixtures

$$\Pi_i = \frac{K_i}{(K_1x_1/\Pi_1^0) + (K_2x_2/\Pi_2^0) + \ldots + (K_nx_n/\Pi_n^0)};$$
$$i = 1, 2, \ldots, n; \quad \text{correlations dominant} \tag{19}$$

The permeation selectivity in the correlations dominant is

$$S_{perm} = \frac{\Pi_i}{\Pi_j} = \frac{K_i}{K_j}; \quad \text{correlations dominant} \tag{20}$$

Eq. (20) shows that when correlations are dominant, the differences in the diffusivities of the component species are washed out and the permeation selectivity is governed purely by the adsorption selectivity.

3. Illustrative examples

To illustrate the application of the simplified analytic expressions derived above, let us consider permeation of CH_4–H_2 mixtures across a ZIF-8 membrane at a temperature $T = 300$ K. The parameter values, estimated on the basis of the data in Ref. [6], are: porosity, $\phi = 0.476$; thickness, $\ell = 40\,\mu$m; diffusivities $Đ_1 = 5 \times 10^{-11}$ m^2 s^{-1}; $Đ_1 = 7.5 \times 10^{-9}$ m^2 s^{-1}; Langmuir parameters, $b_1 = 4.43 \times 10^{-7}$ Pa^{-1}; $b_2 = 1.71 \times 10^{-8}$ Pa^{-1}; saturation capacities, $c_{1,sat} = 18.5$ kmol m^{-3}; $c_{2,sat} = 37$ kmol m^{-3}. To begin with we analyse the ZIF-8 membrane performance with the assumption that nothing is known about the degree of correlations.

The dashed and continuous lines in Fig. 4a represent the calculations of S_{perm} using Eqs. (16) and (20). The correlations negligible scenario yields $S_{perm} = 0.082$, showing that the membrane will be H_2-selective. At the other extreme, in the correlations dominant scenario, $S_{perm} = 12.4$, i.e. the membrane will be CH_4-selective. Also shown in Fig. 4a are the calculations using an exact numerical solution for varying degrees of correlations for each species: $Đ_i/Đ_{ii} = 0.2\theta_i$, $1.0\theta_i$, $10\theta_i$ and $100\theta_i$, whereby we take cater for a linear dependence of the degrees of correlations on the fractional occupancy θ_i, on the basis of the data such as that presented in Fig. 3. The $Đ_{12}$ is determined using the interpolation formula given by Eq. (4). The exact numerical solutions, obtained using the procedures described in our earlier work [21], lie between the two extreme scenarios. The strong influence of correlations on S_{perm} is evident, and the data demonstrate that by increasing the degree of diffusional correlations within the pores, we can reverse the selectivity of the membrane.

Correlations have the effect of slowing down the more mobile H_2. To underline this, Fig. 4b presents the calculations of the permeance of H_2 for three different values of the degrees of correlations for each species: $Đ_i/Đ_{ii} = 0.2\theta_i$, $1.0\theta_i$, $10\theta_i$ and $100\theta_i$. The H_2 permeance is reduced by two orders of magnitude with increasing degree of correlations. With increasing upstream pressure, p_t, the permeance also decreases because of increased occupancy and correlations. The simplified expressions in Eqs. (15) and (18) provide the upper and lower bounds for the permeance of hydrogen.

The windows separating the cages of ZIF-8 are 0.34 nm in size, and only one molecule at a time can hop between cages; therefore the correlation effects are expected to be negligibly small. In this regard the correlation characteristics of ZIF-8 is similar to that of LTA, and CHA. Indeed, the experimental data of Bux et al. [23], obtained with upstream pressures varying between 0.1 and 0.2 MPa, show that the ZIF-8 membrane is H_2-selective. Their experimental data also show that the permeance of H_2 in the mixture is only 15% lower than the unary permeance value. This indicates that the correlations negligible scenario is a reasonable approximation.

If we need the membrane to be CH_4-selective we should choose carbon nanotubes, MFI or mesoporous membranes, ensuring that $Đ_1/Đ_{12}$ is large [6,24].

The correlations negligible scenario is also a good approximation for cage-type zeolites such as CHA, DDR, LTA, TSC, ERI, ITQ-29 that consist of cages separated by 8-ring windows of dimensions in the 3.6–4.2 Å range [10,17,25,26]. To illustrate this we consider the data on the permeance of CO_2 across a SAPO-34 membrane. SAPO-34 is a structural analog of CHA zeolite with a window dimension of 3.77 Å [26], and we expect the diffusion of CO_2 to be practically uncorrelated to its partner species. Fig. 5 presents the data of Li et al.

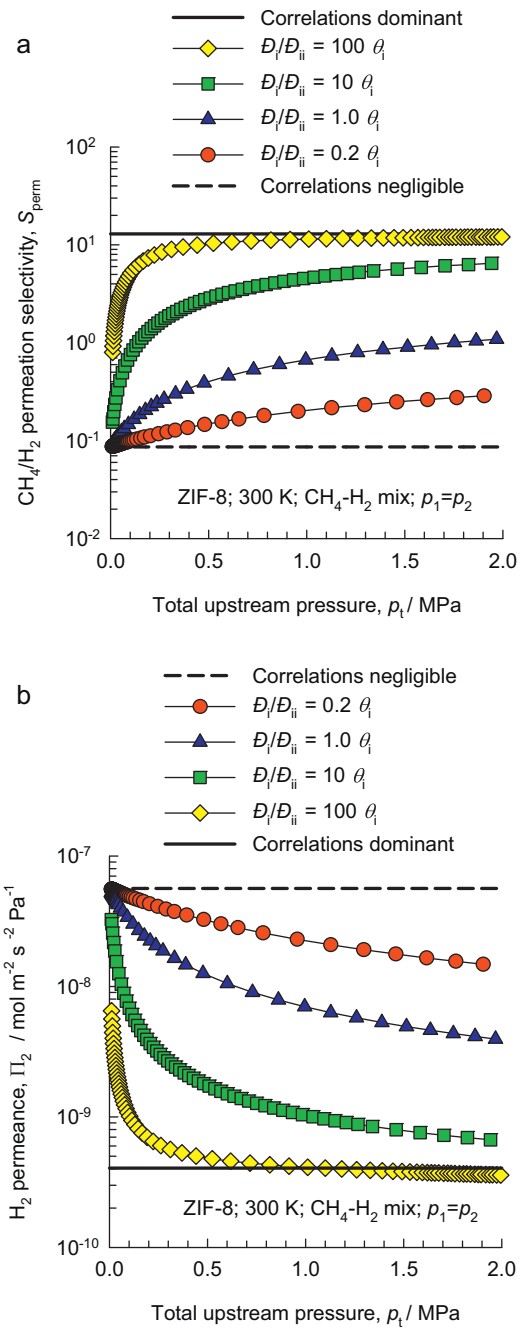

Fig. 4. Comparison of the (a) membrane permeation selectivity, S_{perm}, and (b) permeance Π_i of H_2 for CH_4–H_2 mixture diffusion across ZIF-8 at 300 K for three different values of $0.2\theta_i$, $1.0\theta_i$, $10\theta_i$ and $100\theta_i$. The exchange coefficient $Đ_{12}$ is calculated using the interpolation formula given by Eq. (4). The symbols show the calculations using an exact numerical solution of the M–S equations, along with single-site Langmuir adsorption equilibrium. The dashed and continuous lines represent the correlations negligible and correlations dominant scenario calculations. In these calculations the upstream partial pressures are taken to be equal, $p_1 = p_2$.

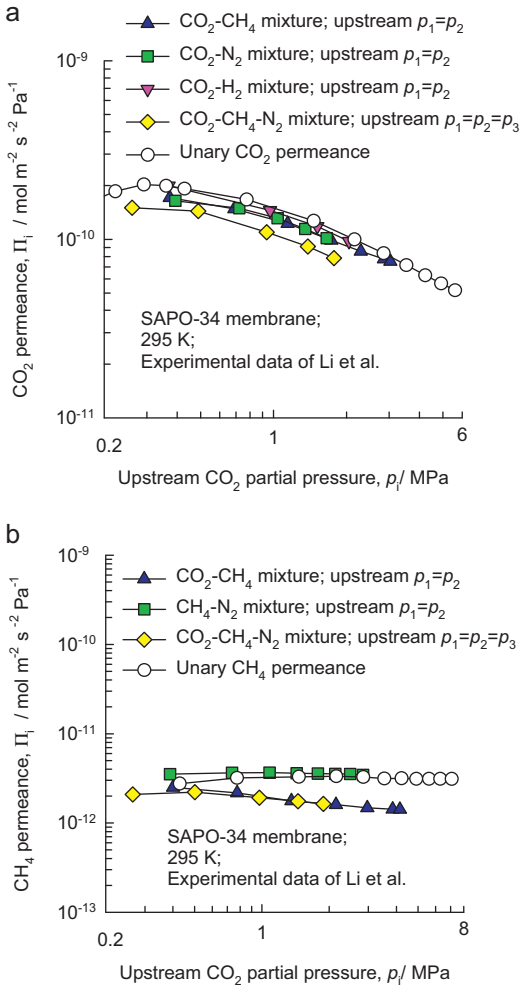

Fig. 5. Data of Li et al. [27] on the permeances Π_i of (a) CO_2, and (b) CH_4 across a SAPO-34 membrane at 295 K, as a function of the upstream partial pressures. The unary permeance is compared with permeances in equimolar CO_2–CH_4, CO_2–N_2, CO_2–H_2, CH_4–N_2, and CO_2–CH_4–N_2 mixtures.

[27] on the permeances Π_i of (a) CO_2, and (b) CH_4 across a SAPO-34 membrane at 295 K, as a function of the upstream partial pressures. The unary permeances of both CO_2 and CH_4 are found to have values close to their permeances in CO_2–CH_4, CO_2–N_2, CO_2–H_2, CH_4–N_2, and CO_2–CH_4-N_2 mixtures, confirming that Eq. (15) is a good approximation.

In order to illustrate an application of the correlations dominant scenario described by Eqs. (19) and (20), let us consider the experimental data presented by White et al. [28] for separation of CO_2 (1) and N_2 (2) using an ultrathin NaY membrane. From Table 1 of White et al. [28], the pure component permeance data for membrane B at 303 K are $\Pi_1^0 = 9.6 \times 10^{-8}$; $\Pi_2^0 = 5.1 \times 10^{-9}$ mol m^{-2} s^{-1} Pa^{-1}. For predictions of the permeation selectivity, S_{perm}, data on adsorption equilibrium is required; this is not provided in White et al. [28]. For this purpose, we carried out Configurational-Bias Monte Carlo (CBMC) simulations of the adsorption equilibrium for CO_2/N_2 mixtures in NaY using the force field and simulation techniques as described in our previous papers [6,29]. The CBMC data on the K_i are presented in Fig. 6a. It is important to note that though the data on the K_i are not constant beyond the Henry regime, the ratio K_1/K_2 is practically independent of pressure. Combining this information with the data on unary permeances, the predictions of S_{perm}, for the two limiting scenarios are shown in Fig. 6b. The experimentally observed value of $S_{perm} = 503$ is in good agreement with that anticipated by the dominant correlations scenario. This result is to be expected because diffusional correlations are strong within NaY [6]. For CO_2/N_2 separation, it is essential to choose a pore topology and pore size that yields extremely high degree of correlations. Structures such as LTA, CHA, DDR and ZIF-8 are not suitable for this separation.

For transport of a variety of mixtures across MFI membranes the correlation effects cannot be ignored, as has been demonstrated in the published literature [7,21]. The correlation dominant scenario provides a good description of mixture diffusion in MFI, especially at high pore concentrations [17].

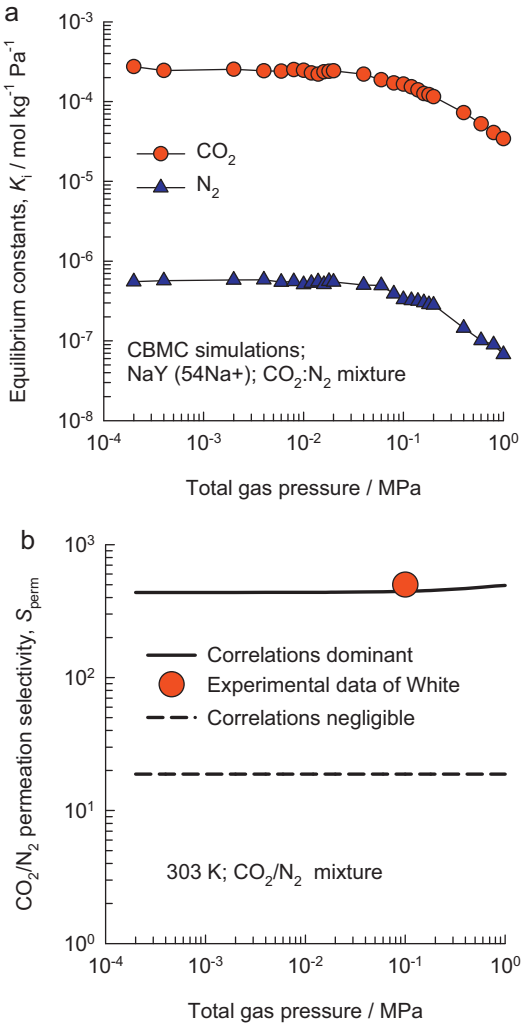

Fig. 6. (a) Configurational-Bias Monte Carlo simulations of the equilibrium constants K_i for CO_2/N_2 adsorption in NaY at 303 K. (b) Calculation of the membrane permeation selectivity, S_{perm}, using Eqs. (15) and (18), along with unary permeances determined experimentally by White et al. [28].

4. Conclusions

Using the Maxwell–Stefan equations as a basis, we have derived simplified expressions for fluxes and permeances of binary mixtures. Two limiting scenarios have been identified. For the correlations negligible scenario, the working expressions for the permeances and permeation selectivities are given by Eqs. (15) and (16). For the correlations dominant scenario, the corresponding expressions for the permeances and permeation selectivities are given by Eqs. (18) and (20). The results of this study underline the strong influence of diffusional correlations on the mixture permeances; these effects can be strong enough to cause a reversal of selectivity.

The developed simplified procedure is particularly useful for preliminary screening purposes. For more accurate designs, the more accurate models described in earlier work [21,22,30] need to be used.

Acknowledgements

This material is based upon work supported as part of the Center for Gas Separations Relevant to Clean Energy Technologies, an Energy Frontier Research Center funded by the U.S. Department of Energy, Office of Science, Office of Basic Energy Sciences under Award Number DE-SC0001015.

Nomenclature

b_i	parameter in the pure component Langmuir adsorption isotherm, Pa^{-1}
$[B]$	matrix of inverse M–S coefficients, defined by Eq. (7), m^{-2} s
c_i	pore concentration of species i, mol m^{-3}
$c_{i,sat}$	saturation capacity of species i, mol m^{-3}
c_t	total pore concentration in mixture, mol m^{-3}
$Đ_i$	M–S diffusivity of species i, m^2 s^{-1}
$Đ_{ij}$	M–S exchange coefficient, m^2 s^{-1}
$Đ_{ij,fl}$	M–S diffusivity in binary i–j fluid mixture, m^2 s^{-1}
F	factor defined by $F \equiv Đ_{ij}/Đ_{ij,fl}$, dimensionless
$[I]$	identity matrix, dimensionless
K_i	Henry coefficient for species i, mol m^{-3} Pa^{-1}
ℓ	thickness of membrane, m
p_i	partial pressure of species i in upstream compartment, Pa
p_t	total system pressure in upstream compartment, Pa
n	number of components in mixture, dimensionless
N_i	molar flux of species i defined in terms of the membrane area, mol m^{-2} s^{-1}
R	gas constant, 8.314 J mol^{-1} K^{-1}
S_{perm}	permeation selectivity, dimensionless
T	absolute temperature, K
x_i	mole fraction of species i based on loading within pore, dimensionless

Greek letters

δ_{ij}	Kronecker delta, dimensionless
$[\Delta]$	matrix defined by Eq. (9), m^2 s^{-1}
Δ_{ij}	elements of $[\Delta]$, m^2 s^{-1}
$[\Gamma]$	matrix of thermodynamic factors, dimensionless
Γ_{ij}	element of $[\Gamma]$, dimensionless
ϕ	fractional pore volume, dimensionless
Π_i	permeance of species i in mixture mol m^{-2} s^{-1} Pa^{-1}
Π_i^0	permeance of pure component i, mol m^{-2} s^{-1} Pa^{-1}
μ_i	molar chemical potential, J mol^{-1}
θ_i	fractional occupancy of component i, dimensionless

Subscripts

i	referring to component i
j	referring to component j
sat	referring to saturation conditions
t	referring to total mixture

Superscripts

0	referring to pure component

Vector and matrix notation

()	component vector
[]	square matrix

References

[1] A.U. Czaja, N. Trukhan, U. Müller, Industrial applications of metal–organic frameworks, Chem. Soc. Rev. 38 (2009) 1284–1293.
[2] J.R. Li, R.J. Kuppler, H.C. Zhou, Selective gas adsorption and separation in metal–organic frameworks, Chem. Soc. Rev. 38 (2009) 1477–1504.
[3] G. Férey, C. Serre, Large breathing effects in three-dimensional porous hybrid matter: facts, analyses, rules and consequences, Chem. Soc. Rev. 38 (2009) 1380–1399.
[4] J. Gascon, F. Kapteijn, Metal–organic framework membranes—high potential, bright future? Angew. Chem. Int. Ed. 49 (2010) 1530–1532.
[5] J. Caro, M. Noack, Zeolite membranes—recent developments and progress, Micropor. Mesopor. Mater. 115 (2008) 215–233.

[6] R. Krishna, J.M. van Baten, In silico screening of zeolite membranes for CO_2 capture, J. Membr. Sci. 360 (2010) 323–333.
[7] J.M. van de Graaf, F. Kapteijn, J.A. Moulijn, Modeling permeation of binary mixtures through zeolite membranes, AIChE J. 45 (1999) 497–511.
[8] J.A. Sheffel, M. Tsapatsis, A semi-empirical approach for predicting the performance of mixed matrix membranes containing selective flakes, J. Membr. Sci. 326 (2009) 595–607.
[9] R. Krishna, J.M. van Baten, Unified Maxwell–Stefan description of binary mixture diffusion in micro- and meso-porous materials, Chem. Eng. Sci. 64 (2009) 3159–3178.
[10] R. Krishna, Describing the diffusion of guest molecules inside porous structures, J. Phys. Chem. C 113 (2009) 19756–19781.
[11] G.R. Gavalas, Diffusion in microporous membranes: measurements and modeling, Ind. Eng. Chem. Res. 47 (2008) 5797–5811.
[12] R. Krishna, J.M. van Baten, Highlighting pitfalls in the Maxwell–Stefan modeling of water–alcohol mixture permeation across pervaporation membranes, J. Membr. Sci. 360 (2010) 476–482.
[13] R. Krishna, J.M. van Baten, Segregation effects in adsorption of CO_2 containing mixtures and their consequences for separation selectivities in cage-type zeolites, Sep. Purif. Technol. 61 (2008) 414–423.
[14] R. Krishna, J.M. van Baten, Mutual slowing-down effects in mixture diffusion in zeolites, J. Phys. Chem. C 114 (2010) 13154–13156.
[15] R. Krishna, J.M. van Baten, Insights into diffusion of gases in zeolites gained from molecular dynamics simulations, Micropor. Mesopor. Mater. 109 (2008) 91–108.
[16] R. Krishna, J.M. van Baten, Onsager coefficients for binary mixture diffusion in nanopores, Chem. Eng. Sci. 63 (2008) 3120–3140.
[17] R. Krishna, J.M. van Baten, Describing mixture diffusion in microporous materials under conditions of pore saturation, J. Phys. Chem. C 114 (2010) 11557–11563.
[18] R. Krishna, J.M. van Baten, Investigating cluster formation in adsorption of CO_2, CH_4, and Ar in zeolites and metal organic frameworks at sub-critical temperatures, Langmuir 26 (2010) 3981–3992.
[19] R Krishna, J.M. van Baten, Highlighting a variety of unusual characteristics of adsorption and diffusion in microporous materials induced by clustering of guest molecules, Langmuir 26 (2010) 8450–8463.
[20] R. Krishna, J.M. van Baten, Hydrogen bonding effects in adsorption of water–alcohol mixtures in zeolites and the consequences for the characteristics of the Maxwell–Stefan diffusivities, Langmuir 26 (2010) 10854–10867.
[21] R. Krishna, R. Baur, Modelling issues in zeolite based separation processes, Sep. Purif. Technol. 33 (2003) 213–254.
[22] R. Krishna, R. Baur, Analytic solution of the Maxwell–Stefan equations for multicomponent permeation across a zeolite membrane, Chem. Eng. J. 97 (2004) 37–45.
[23] H. Bux, F. Liang, Y. Li, J. Cravillon, M. Wiebcke, J. Caro, Zeolitic imidazolate framework membrane with molecular sieving properties by microwave-assisted solvothermal synthesis, J. Am. Chem. Soc. 131 (2009) 16000–16001.
[24] H.B. Chen, D.S. Sholl, Predictions of selectivity and flux for CH_4/H_2 separations using single walled carbon nanotubes as membranes, J. Membr. Sci. 269 (2006) 152–160.
[25] R. Krishna, J.M. van Baten, Comment on "modeling adsorption and self-diffusion of methane in LTA zeolites: the influence of framework flexibility", J. Phys. Chem. C 114 (2010) 18017–18021.
[26] R. Krishna, J.M. van Baten, A molecular dynamics investigation of the diffusion characteristics of cavity-type zeolites with 8-ring windows, Micropor. Mesopor. Mater. 137 (2011) 83–91.
[27] S. Li, J.L. Falconer, R.D. Noble, R. Krishna, Interpreting unary, binary and ternary mixture permeation across a SAPO-34 membrane with loading-dependent Maxwell–Stefan diffusivities, J Phys. Chem. C 111 (2007) 5075–5082.
[28] J.C. White, P.K. Dutta, K. Shqau, H. Verweij, Synthesis of ultrathin zeolite Y membranes and their application for separation of carbon dioxide and nitrogen gases, Langmuir 26 (2010) 10287–10293.
[29] A. García-Sánchez, C.O. Ania, J.B. Parra, D. Dubbeldam, T.J.H. Vlugt, R. Krishna, S. Calero, Development of a transferable force field for carbon dioxide adsorption in zeolites, J. Phys. Chem. C 113 (2009) 8814–8820.
[30] R. Krishna, S. Li, J.M. van Baten, J.L. Falconer, R.D. Noble, Investigation of slowing-down and speeding-up effects in binary mixture permeation across SAPO-34 and MFI membranes, Sep. Purif. Technol. 60 (2008) 230–236.
[31] R. Krishna, J.M. van Baten, An investigation of the characteristics of Maxwell–Stefan diffusivities of binary mixtures in silica nanopores, Chem. Eng. Sci. 64 (2009) 870–882.